行政院國家科學委員會專題研究計畫　期中進度報告

椎間盤受連續性載荷時之動態分析及其在評估人工椎間核功能之應用(1/2)

計畫類別：個別型計畫
計畫編號：NSC92-2320-B-002-103-
執行期間：92 年 08 月 01 日至 93 年 07 月 31 日
執行單位：國立臺灣大學醫學工程學研究所

計畫主持人：王兆麟

報告類型：精簡報告
報告附件：出席國際會議研究心得報告及發表論文
處理方式：本計畫可公開查詢

中　華　民　國 93 年 5 月 26 日

行政院國家科學委員會專題研究計畫 期中進度報告
椎間盤受連續性載荷時之動態分析及其在評估人工椎間核功能之應用
(1/2)

計畫編號：NSC 92－2320－B－002－103

執行期間：92 年 08 月 01 日 至 93 年 07 月 31 日

計畫主持人：王兆麟

臺灣大學醫學暨工學院醫學工程學研究所

由於本計畫之執行，已有兩篇研討會論文發表，與四篇期刊論文（一篇審查中，三篇準備中），成果堪稱豐碩。以下是論文目錄以及部份論文內容。

研討會論文

1. Lai CC, **Wang JL,** Chang GL, Chung CH, The load sharing contribution of spinal facet joint during impact loading – a porcine biomechanical model, ASME International Mechanical Engineering Congress and R&D Expo (IMECE), 2003, Paper No. IMECE2003-42940. (見附件)
2. **Wang JL,** Chung CH, Lai CC, Chang CC, The variation of gross force response of spinal motion segment during cyclic loading – a porcine biomechanical model, ASME International Mechanical Engineering Congress and R&D Expo (IMECE), 2003, Paper No. IMECE2003-42939.

期刊論文

1. **Wang JL,** Tsai YC, Yang BD. Strain energy density distribution of vertebral body of two motion segment model under combined compression and sagittal bending moment – an in vitro porcine spine biomechanical study. Submitted for Journal of the Chinese Institute of Engineers. (見附件)
2. **Wang JL,** Tsai YC, Yang BD. The strain field of vertebral body under combined compression and sagittal bending moment. Under preparation.
3. **Wang JL**, Lai CC, Chang GL, Chung CH. The facet joint loading of spinal motion segment under pointed compressive impact loading – A biomechanical in vitro porcine model. Under preparation.
4. **Wang JL**, Chang CH. An innovative instrument in measuring the intra-disc pressure under combined compression and sagittal bending moment – And the effect of locations of sensor insertion. Under preparation.

Proceedings of IMECE'03
2003 ASME International Mechanical Engineering Congress & Exposition
Washington, D.C., November 16-21, 2003
IMECE2003-42940

THE LOAD SHARING CONTRIBUTION OF SPINAL FACET JOINT DURING IMPACT LOADING – A PORCINE BIOMECHANICAL MODEL

Cheng-Chuan Lai[2], Jaw-Lin Wang[1], Guan-Liang Chang[2], Cheng-Hsien Chung[1]
[1]Institute of Biomedical Engineering, National Taiwan University, Taipei, Taiwan
[2]Institute of Biomedical Engineering, National Cheng Kung University, Tainan, Taiwan

ABSTRACT

The components that share the loading of motion segment include the facet joint and disc. Nachemson [1] reported the facet joint share 18% of vertical loading in a motion segment; while many other researchers reported the load sharing percentage of facet joint ranges from 1% to 57% [2,3]. The current study developed a unique apparatus using an in vitro porcine spine model to quantify the alteration of loading in the facet joint under impact compressive loading at different loading conditions. A drop tower type impact apparatus was used to produce the impact energy for the motion segment. A 6-D load cell was placed under the specimen to detect the force and moment responses. The pressure sensor was inserted into the facet joint to find the contact force. The pointed axial compressive forces were applied at 8 locations from anterior to posterior of upper vertebrae to mimic different impact loading conditions. The impact energy was fixed at 1.2 J. We found that; when the loading was applied anteriorly, the facet joint sustained very small percentages of the loading; while the location of the loading moved posteriorly, the facet joint sharing percentages increased. The largest sharing percentages of facet joint reached 30% in the current study.

MATERIALS AND METHODS

Three fresh-frozen porcine spinal motion segment (L2/L3) was used in the experiment. The specimens were dissected preserving the osteoligamentous structure. A "drop-tower type" impact testing apparatus was modified for the testing (Figure 1). The impactor was guided by two rods to give a vertical motion. The energy was transmitted to the specimen through the impounder. The shock absorber was placed on the top of the impounder to control the impact contact period. The stiffness of shock absorbers is 180 kN/m when the loading speed is 1.4 m/sec. The shock absorber is able to give, approximately, the contact time of impact at levels of 40 mini-seconds when testing a standard rubber bar specimen (Stiffness = 1000 kN/m, Length = 110 mm) at 12 kg impact mass and 50 mm impact height. The fixed frame, which is fixed to the guiding rode, is used to align the vertical movement of impounder. The specimen was mounted vertically below the impounder with a uni-axial load cell (Kistler 9021A, Kistler Instrumente, Winterthur, Switzerland) and above the six-axial force load cell (AMTI MC6-6-4000, Advanced Mechanical Technology, Inc., Watertown, MA, USA). An LVDT (ACT500A, RDP Electronics Ltd., Health Town, Wolverhampton, UK) was applied on the impounder to check the deformation of specimen. The specimen was loaded at eight points from anterior to posterior. Each loading point is 10 mm apart. The trajectory of the vertical loading of point 1 is along the anterior wall of vertebrae, while that of point 3 and point 4 enter the central of vertebrae. The loading trajectory of point 5 is along the posterior wall, and that of point 7 and 8 goes through the facet joint (Figure 2). The impact height is 10 mm, and the impact weight is 12 kg; hence the impact energy is 1.2 J. The pressure sensors (FlexiForce Sensors, Model#A101, Tekscan Inc.) were inserted into the both facet joints to find the joint contact force. Signals of facet joint contact force, input force, three dimensional reaction forces and moments from the six-axial force load cell were all recorded at 10 kHz sampling frequency. The signals were than low pass filtered at 500 Hz frequency using Butterworth filtering algorithm.

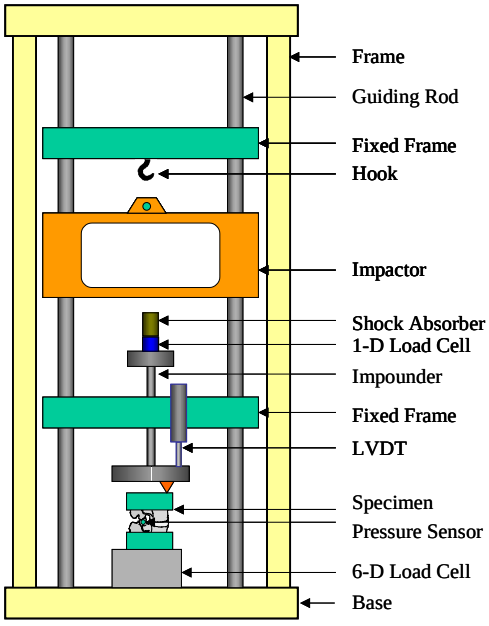

Figure 1. The schematic plot of testing apparatus. The vibrator was guided by two rods to give a vertical motion. The energy of the vibration was produced with the two eccentric rotors. The specimen was mounted vertically below the impounder and above the six-axial force load cell.

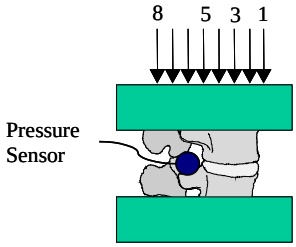

Figure 2. Schematic plot of loading locations of spine joint

RESULTS

The typical loading history of axial force, bending moment and total joint contact pressure of selected points at point 1 (anterior), point

4 (central), and point 7 (posterior) of specimen #2 were plotted in Figure 3. The impact contact time is controlled within 40 mini-seconds, and the peak loading is around 600 N (Figure 3A). The bending moment varies largely with respect to the loading point. The moment was in flexion when the load was applied at the anterior of vertebral body, and was in extension when the load was applied posteriorly (Figure 3B). The facet joint force was small when the loading was applied anteriorly, but responded promptly with the axial force when the loading was applied posteriorly (Figure 3C). The axial resultant force remained constant w.r.t. the variation of loading locations. The facet joint contact force increased, but the flexion moment decreased when the loading locations moved posteriorly (Figure 4). When the loading was applied anteriorly, the facet joint sustained very small percentages of the loading; while the location of the loading moved posteriorly, the facet joint sharing percentage increased. The largest sharing percentages of facet joint reached 30% (Figure 5).

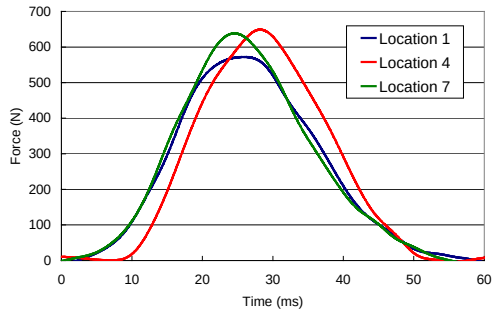

(A)

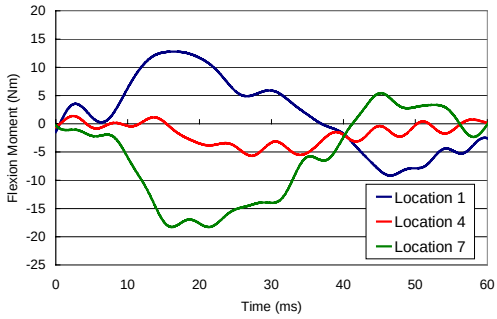

(B)

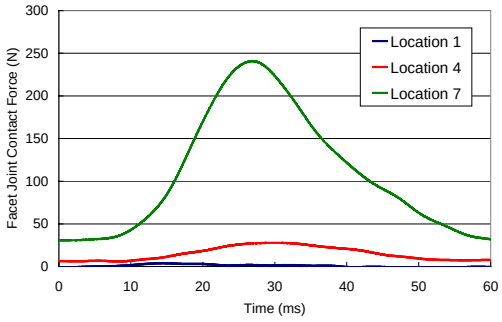

(C)

Figure 3. The (A) axial force, (B) bending moment and (C) total facet joint contact force of specimen loaded at location 1 (anterior), 4 (central), & 7 (posterior)

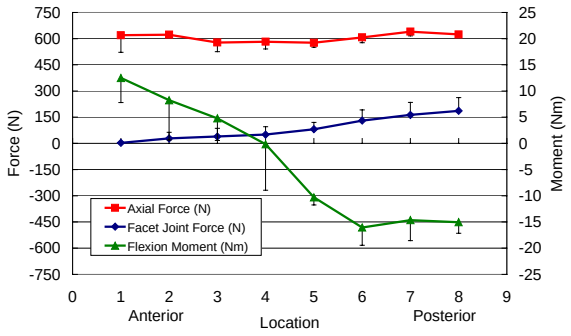

Figure 4. The peak axial and facet joint force, and the flexion bending moment with respect to the location of loading point.

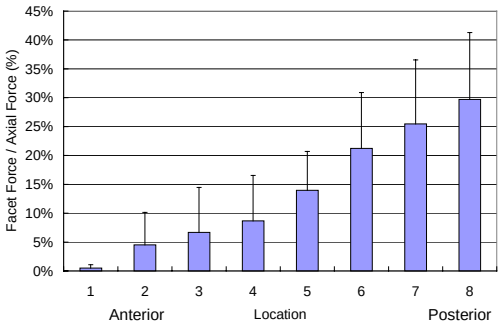

Figure 5. The sharing percentages of facet joint over the axial resultant force.

DISCUSSION

We successfully developed an apparatus that is able to detect the three dimension dynamic forces, moments and facet joint contact force responses of testing specimens during impact loading. We showed that the value of maximum moment and facet joint contact force responses of spine joint was determined not only by the magnitude of axial loading but also the loading locations. The load sharing of fact joint of current study ranges from 0 to 30%, which is close to the prediction of Nachemson's results [1]. However, our results give a more detail inspection on the effect of loading condition. The limitation of current study is the geometric inconsistency of porcine spine from human spine. The anatomic variation of porcine spine with respect to human one will be studied, and the relationship of facet joint geometry and loading condition need to be verified in the future.

REFERENCES

[1] Nachemson A (1960) Acta Orthop Scandinav Supp, 43: 1-104.
[2] Adams MA, Hutton WC (1980) J Bone Joint Surg, 62B: 358-362.
[3] Lorenz M, Patwardhan A, Vanderby. (1983) Spine, 8: 122-130.

ACKNOWLEDGEMENT

We acknowledge the financial support of the National Science Council, ROC, NSC 91-2320-B-002-159.

STRAIN ENERGY DENSITY DISTRIBUTION OF VERTEBRAL BODY OF TWO MOTION SEGMENT MODEL UNDER COMBINED COMPRESSION AND SAGITTAL BENDING MOMENT – AN IN VITRO PORCINE SPINE BIOMECHANICAL STUDY

Jaw-Lin Wang, Ph.D. and Yuan-Chuan Tsai, B.S., Been-Der Yang, Ph.D.
Institute of Biomedical Engineering, College of Medicine and College of Engineering,
National Taiwan University

ABSTRACT

The purpose of current study is to find the strain energy density (SED) distribution of vertebral body during different compression loading combined with sagittal bending moment. The combined flexion and extension, which is generated by applying an eccentric pointed loading on the motion segment, is to mimic different postures of trunk and loading on the spine column. Two strain gage rosettes were applied at the anterior site and posterior site of vertebral body. The total SED, deviatoric SED and dilatation SED were obtained from the measurement of two rosettes. Three major phenomena are observed in the current study; first, the anterior site of vertebra is at higher risk comparing to the posterior site of vertebra when the motion segment is in compression combined with extreme flexion and extension. Second, the SED is minimal when the loading is applied along the trajectories of spinal cannel and facet joint. Third, the major contribution of SED is from the deviatoric SED. The distribution of SED within the vertebral body during different loading condition can serve as the baseline of treatment in preventing the vertebral body from the risk of compression fracture.

Key Words: Strain Energy Density, Vertebral Body, Spine Biomechanics

1. INTRODUCTION

The principle of traditional spinal fixation instruments is to provide strong fixation and stability of two adjacent moving vertebral bodies. That is to restore the posture and stiffness before trauma or injury occurs. It is hence essential to find normal posture and stiffness of intact motion segment. The well-recognized method of evaluating the spine function is to apply the pure moment on the motion segment, and then measure the relative rotation of two vertebras. The larger relative rotation indicates the less stability, and vice versa (Abumi et al. 1989; Panjabi 1988; Panjabi et al. 1988; Wilke et al. 1998). Although this evaluation method is straightforward, it only provides the global biomechanical behavior of motion segment. The resolution of traditional stability test cannot differentiate the outcome of the newly developed technique, for instance, the percutaneous vertebroplasty (PV) treatment. The PV treatment is used to recover the strength of vertebra. The local biomechanical behavior, e.g. bone strain, stress and strain energy density (SED), needs to be observed to find the subtle changes with respect to the treatment. It is therefore important to find the micro mechanics of vertebra such as strain, stress and SED of normal condition as the baseline for the study of PV treatment.

The strain gage implantation on the surface of bone was widely used for the study of in vivo loading and bone growth and adaptation (Burr et al. 1985; Burr et al. 1989a; Burr et al. 1989b; Lanyon and Rubin 1984; Rubin and Lanyon 1984). The strain gage rosettes can also be used to measure the strain field and calculate SED. An in vivo measuring of human tibia showed that the SED reached 0.5 kJ/m^3 and 5.5 kJ/m^3 during walking and jogging, respectively (Mikic and Carter 1995). In addition, he found, during a gait cycle, the majority contribution of SED at heel-off stage came from the shear SED. A maximum of 54 kJ/m^3 SED was found on the equine third metacarpal midshaft throughout the stance and swing phase (Gross et al. 1992). Nevertheless, the application of strain gage on spine biomechanics is limited to the measurement of strain of the vertebral body (Frei et al. 2002; Frei et al. 2001; Hongo et al. 1999; Shah et al. 1978) and the contact force of the facet joint (Buttermann et al. 1991; Buttermann et al. 1992) only. The strain measurement of vertebral body was used to find the stress concentration of vertebral body during impact burst fracture (Hongo et al. 1999). Hongo et al. attached 11 gages on the surface cortical bone, and applied the axial compressive loading on the top of vertebral body. They found the posterior site of the vertebra was the most critical site for burst fracture injury.

The aim of current study is to find the distribution of SED of vertebra during different compression loading combined with sagittal bending moment. The motion segment is pointed compressive loaded to mimic the motion segment at different postures or rehabilitation strategies. For example, when the pointed load is applied along the trajectory of anterior wall of vertebral body, it mimics the combined flexion loading together with the compressive loading. When the load is applied along the trajectory of posterior process, it mimics the combined extension together with the compressive loading. In this study, we are interested in compression fracture injury; hence, the total SED, together with the deviatoric and volumetric SED at anterior and posterior site are measured. It is hoped we can find the subtle changes in the vertebra during different loading condition. The founding of the current study can serve as the

baseline for the future studies in finding the ultimate treatment of the augmentation of vertebral body, such as the PV.

2. METHODS AND MATERIALS

Eight fresh-frozen porcine spinal motion segments (T12/L1/L2) were used in the experiment. The specimens were dissected preserving the osteoligamentous structure. A "drop-tower type" impact testing apparatus was modified for the testing (Figure 1). The impactor was guided by two rods to give a vertical motion. The energy was transmitted to the specimen through the impounder. The shock absorber was placed on the top of the impounder to control the loading contact period. The stiffness of the shock absorber is 180 kN/m when the loading speed is 1.4 m/sec. The shock absorber is able to give, approximately, the contact time at levels of 40 mini-seconds when testing a standard rubber bar specimen (Stiffness = 1000 kN/m, Length = 110 mm) at 12 kg impact mass and 50 mm impact height. The fixed frame, which is fixed to the guiding rode, is used to align the vertical movement of the impounder. The specimen was mounted vertically below the impounder and above the six-axial force load cell (AMTI MC6-6-4000, Advanced Mechanical Technology, Inc., Watertown, MA, USA).

The specimen was loaded at eight points of location from anterior to posterior. Each loading point is 10 mm apart. The trajectory of the vertical loading of point 1 is along the anterior wall of vertebral body, while that of point 2 enters the central of vertebral body. The loading trajectory of point 3 is along the posterior wall, and that of point 4 and 5 go through the spinal cannel and facet joint. The trajectory of point 6, 7 and 8 go through the posterior process (Table 1 & Figure 2). The loading height is 10 mm, and the weight is 12 kg; hence the input energy is 1.2 J. Two 3-axial strain gage rosettes (Kyowa KFG-1-120-D17-11N50C2, Kyowa Electronics Instruments Co., Ltd., Tokyo, Japan) were applied on the anterior and posterior site of vertebral body (Figure 3). Signals of two strain gage rosettes, resultant axial forces and flexion moments were recorded at 10 kHz sampling frequency. The signals were then low pass filtered at 500 Hz frequency using Butterworth filtering algorithm.

The two principal strains at anterior and posterior site of vertebral body can be calculated from the measurement of two strain gage rosettes. The total, dilatation and deviatoric SED can be obtained from the two principal strains and stresses using the following equations.

$$SED_{total} = \frac{E}{2(1-\upsilon^2)}(\varepsilon^2{}_1 + \varepsilon^2{}_2 + 2\upsilon\varepsilon_1\varepsilon_2)$$

$$SED_{dilatation} = \frac{1-2\upsilon}{6E}(\sigma_1 + \sigma_2)^2$$

$$SED_{deviatoric} = SED_{total} - SED_{dilatation}$$

where E=11.032 GPa, ν = 0.3 for cortical bone (Cao et al. 2001). The stiffness of cortical bone is assumed to be isometric.

3. RESULTS

The typical loading history of axial force and bending moment of point 1 (anterior of vertebral body), point 4 (spinal cannel), and point 7 (posterior process) of specimen #11 are plotted in Figure 4. The contact time of loading is controlled within 50 mini-seconds. The peak force reaches around 500 N for this specimen. No significant pattern and magnitude variation of the axial force is found from the changing of loading points (Figure 4A). The pattern of bending moment is, however, changes with the location of loading points. The moment is in flexion when the load is applied at the anterior of vertebral body, and is in extension when the load is applied at the posterior process of motion segment (Figure 4B). The maximum magnitude of axial force and bending moment of each loading with respect to the location of loading points is plotted in Figure 5. The variation of magnitude of axial force is about constant for all points of loading location. The bending moment is in flexion when the load is applied along the trajectory of anterior and center of vertebra. The bending moment is about zero when the load is applied along the trajectory of posterior of vertebra. The extension moment increases as the loading point moves toward the spinal cannel and facet joint. However; the bending moment slightly decreases if the loading moves further to the posterior site of posterior process.

The total, deviatoric and dilatation SED at both anterior and posterior site is highest when the load is applied at anterior wall of vertebral body (point 1) and the very last location of posterior process (point 8), that is the extreme loading condition of axial loading combined with flexion and extension. The SEDs decrease when the loading point gradually approaches the center of motion segment. All the SEDs are smallest when the loading is applied along the spinal canal (point 4) and facet joint (point 5). This may indicate that the vertebra is at least risk when the loading is applied at the center of the motion segment, i.e. the trajectory of the spinal canal and facet joint, but not the center of vertebra. During the extreme loading condition; i.e. the loading point 1, 2, 7, 8; the SEDs at anterior site of vertebra are higher than that of at posterior site, which may indicate that, the anterior site of vertebra encounters more risk than the posterior site when the motion segment is at extreme flexion and extension. The highest total SED is at the order of 10 kJ/m^3, and the lowest total SED is at the order of 1 kJ/m^3 when the input energy of the specimen is 1.2 J (Figure 6).

Around 90% of the total SED is contributed by

the deviatoric SED. At the anterior site of vertebral body, the contribution of deviatoric SED to the total SED is uniformly and slightly above 90% for SED for all points of loading location. At the posterior site of vertebral body, the contribution of deviatoric SED, nevertheless, is smaller when the load is applied at anterior wall of vertebra, i.e. around 85%, but gradually increases when the load is applied at posterior process, i.e. well above 95% (Figure 7).

4. DISCUSSION

To our knowledge, this is the first time that the SED distribution of vertebra with respect to the loading condition was measured. Our results are in the scale of single digit of kJ/m^3, which is consistent to the in vivo SED of human tibia cortex during walking. The input energy of our experiment is only 1.2 J, which is considerably smaller than the in vivo condition. However, since the cross section area and height of specimen is estimated at 2000 mm^2 and 100 mm, and the total volume is in the range of $2*10^{-4}$ m^3. Assuming the average SED within the vertebra to be 5 kJ/m^3. This gives the stored energy within the specimen to be 1 J, which is consistent to scale of input energy. The estimation, therefore, warranted our data.

Three major phenomena are observed in the current study; first, the anterior site of vertebra is at higher risk comparing to the posterior site of vertebra when the motion segment is in compression combined with extreme flexion and extension. Second, the SED is minimal when the loading is applied along the trajectories of spinal cannel and facet joint. Third, the major contribution of SED is from the deviatoric SED. The first phenomenon is consistent with the pathological observation of vertebra compression fracture, i.e. the collapse of anterior vertebral body. The second phenomenon may indicate that the straight posture, which the gravity line of loading trajectory pass through the center of motion segment, is best in minimizing the risk for the vertebral body from the compression fracture. The third phenomenon may imply that the collapse of anterior wall of vertebra could be analogue to the ductile fracture observed in engineering material.

It should be noted that; although we used the impact testing apparatus to conduct the experiment, the current simulation is not for simulation of the burst fracture of vertebra, another common vertebra deformity observed during accidental injury. The major difference of simulation of the two fractures is the configuration of loading condition. The current loading condition is axial point load on the top of vertebra. The motion segment is freely to rotate in the sagittal plane. During the burst fracture, that the occurrence of injury is so fast, the rotation of motion segment in sagittal plane is limited. Hence the simulation of burst fracture is, in general, distributed loaded with the constrained rotation in the sagittal plane (Oda and Panjabi 2001; Oda et al. 2001; Panjabi et al. 2001b; Panjabi et al. 2000). The current protocol is designed to simulate the effect of posture, rehabilitation strategies and daily physiological activities.

The source of in-vitro experiments comes from human and animal. The advantage of using the animal model is the consistence of specimen condition that often leads to small variation of experiments. It is widely used for instrumentation performance (Allan et al. 1990; Nasca et al. 1990; Panjabi 1998; Rikhraj et al. 1999). The calf (Allan et al. 1990; Davies et al. 1984; Wilke et al. 1997; Wilke et al. 1996), swine (Allan et al. 1990; Davies et al. 1984) and sheep (Davies et al. 1984; Wilke et al. 1997) are generally used for in-vitro spine biomechanical testing. The advantage of using the human specimen is that the results reflect the human spine behaviors. However, the research with human specimen generally uses few specimens, and the condition of the specimens varies a lot due to the lack of control on subject's age, gender … etc. The large variation of the human specimen is not good for the statistical analysis; however, it is good to interpret the results, which show the spectrum of mechanical behavior of human specimens (Panjabi 1998). The biomechanical difference of animal from the human specimens includes the material properties and structural morphology.

In this study, we used porcine spine model. We tested the bone quality of porcine vertebral body using dual-energy x-ray absorptiometry (Dexa) scanning. The bone mineral density (BMD) of 92 kg and 120 kg porcine spine ranges from 1.107 to 1.165 g/cm^2 (Mitchell et al. 2001), where the average value of Chinese female from 20 to 50 years of age surveyed at National Taiwan University Hospital range from 1.102 to 1.012 g/cm^2. Our results from porcine vertebra may represent the results of healthy adult before the aging taking effect. Comparing to other experimental animals such as calf, sheep, rabbit, rat, … etc, the morphology of porcine lumbar spine is the one analogous most to the human spine in terms of morphology (McLain et al. 2002). The most significant morphological difference is the structure of the anterior facet joint (analogous to the superior facet joint in human spine), which is a "hook" like process (Figure 8) in comparison to the straight process in human spine. Although this geometric difference may put the facet joint in higher load sharing especially at lateral shear loading, the loading condition of our testing is in axial compression only. It is hence we believe that the effect of the morphological difference in such loading condition can be minimal.

We do not consider the effect of muscle recruitment in this study. Some researchers tried to find the spinal physiological loading by putting the load cell into the internal fixation instrumentation (Graichen et al. 1996; Rohlmann et al. 1994; Rohlmann et al. 1998; Rohlmann et al. 2000); however, the data is still not physiological. Recently, the follower load, which is provided by the tensioned cable along the axis of spinal column, is designed to mimic the stability effect of the muscle (Cripton et al. 2000; Miura et al. 2002; Panjabi et al. 2001a; Patwardhan et al. 2000; Patwardhan et al. 1999; Patwardhan et al. 2001; Rohlmann et al. 2001). In our current study, we focused on the effect of the axial

compressive loading and combined flexion and extension. The effects of other directions of forces and moments are minimal.

The spine testing apparatus can be categorized into the functional (stability) testing apparatus and the traumatic testing apparatus. The purpose of functional testing apparatus is to mimic the physiological loading condition of the human body. The static loading magnitude of the in-vitro testing of lumbar spine is well recognized, e.g. 7.5 to 10 Nm for flexion moment (Panjabi 1988; Panjabi et al. 1988; Wilke et al. 1998), and 800 N to 2 kN for axial loading (Nachemson 1981). The purpose of trauma testing apparatus is to mimic various trauma conditions resulting from accidental, occupational or sports injury, e.g. the burst fracture of thoracolumbar spine (Oda and Panjabi 2001; Oda et al. 2001; Panjabi et al. 2001b), whiplash injury of cervical spine (Panjabi et al. 1998a; Panjabi et al. 1998b; Panjabi et al. 2004), and the repetitive injury of lumbar spine (Au et al. 2001; Yoganandan et al. 1994). Hence the loading magnitude of traumatic testing is in higher order than the physiological loading. We used the vertical pointed loading to generate the complex axial loading combined with sagittal bending moment using the impact testing apparatus developed at our laboratory. In the current test, the highest magnitude of the axial loading is at 600 N, 20 Nm flexion and 25 Nm extension, which are within the range of physiological testing, but not the traumatic testing. This magnitude fits the purpose of simulating motion segment at different postures and rehabilitation strategies.

ACKNOWLEDGEMENT

We appreciate the support from National Science Council of Taiwan, the Republic of China (NSC 92-2320-B-002-103).

Table 1. The anatomic landmark of point of loading locations

Point	1	2	3	4	5	6	7	8
Anatomic landmark	Anterior Center Posterior Vertebral Body			Spinal Cannel	Facet Joint	Posterior Process		

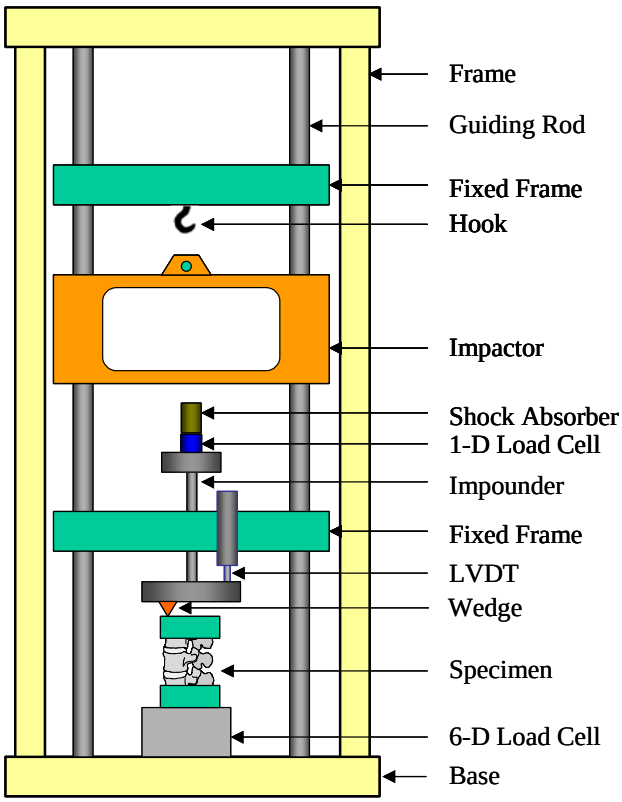

Figure 1. Continuous Impact Testing Apparatus (CITA). The impactor is guided by two rods to give a vertical motion. The specimen is mounted vertically below the impounder and above the six-axial force load cell.

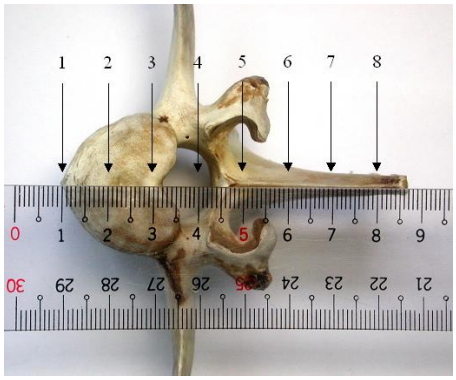

Figure 2. Locations of loading point on the motion segment

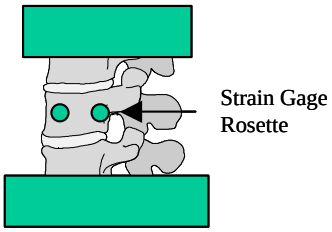

Figure 3. Locations of strain gage rosettes on the vertebral body

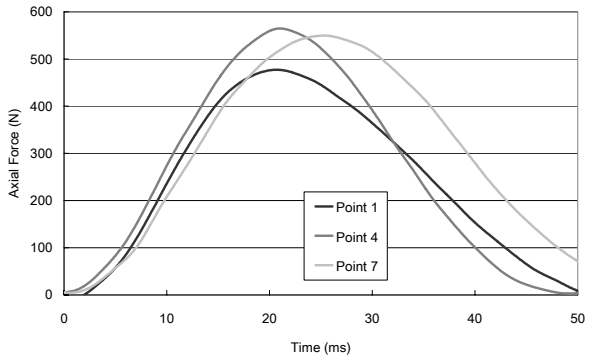

(A)

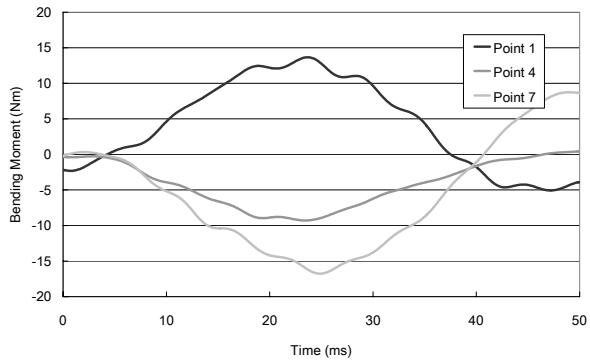

(B)

Figure 4. Typical loading histories of (A) axial force and (B) bending moment of specimen loaded at point 1 (anterior of vertebral body), point 4 (spinal cannel), and point 7 (posterior process).

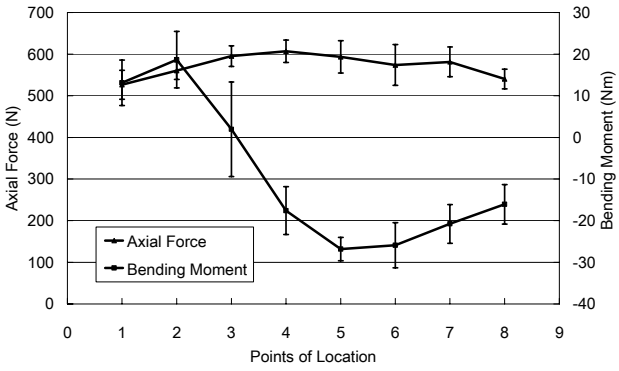

Figure 5. Peak axial force and the flexion bending moment with respect to the location of loading point

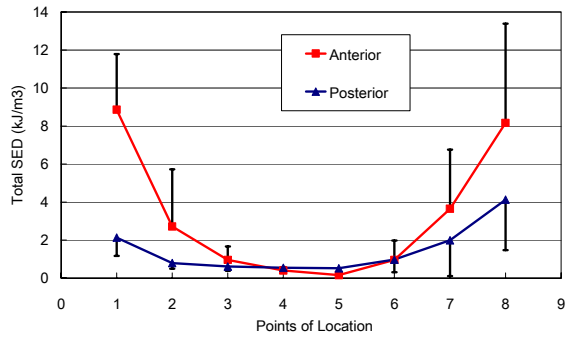

(A)

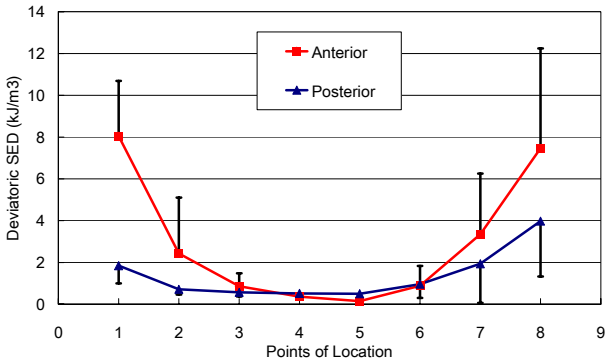

(B)

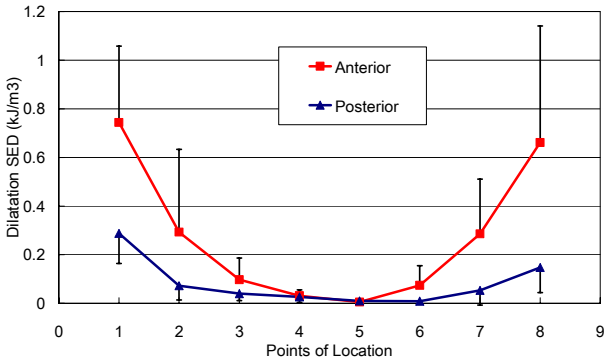

(C)

Figure 6. (A) Total SED, (B) Deviatoric SED, (C) Dilatation SED of vertebral body at anterior and posterior site with respect to the location of loading point

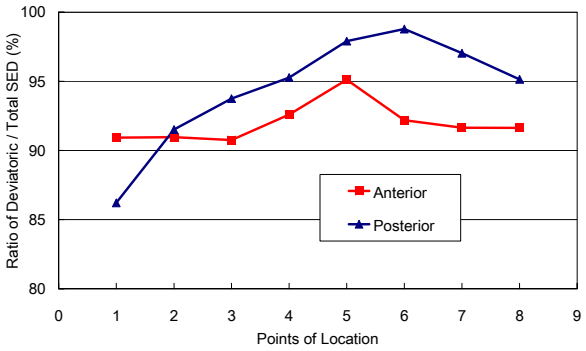

Figure 7. Ratio of deviatoric SED over total SED of vertebral body at anterior and posterior site with respect to the location of loading point

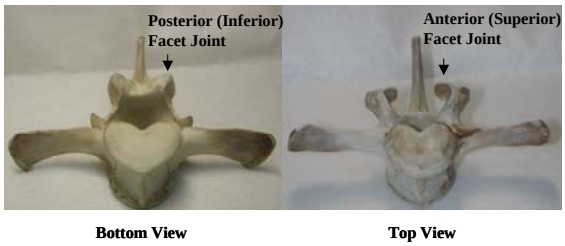

Figure 8. Bottom view and top view of porcine vertebra

REFERENCES

Abumi, K., Panjabi, M., and Duranceau, J., 1989, "Biomechanical evaluation of spinal fixation devices. III. Stability provided by six spinal fixation devices and interbody bone graft," *Spine*, Vol. 14, No., pp. 1249-1255.

Allan, D. G., Russell, G. G., Moreau, M. J., Raso, V. J., and Budney, D., 1990, "Vertebral end-plate failure in porcine and bovine models of spinal fracture instrumentation," *Journal of Orthopaedic Research*, Vol. 8, No. 1, pp. 154-6.

Au, G., Cook, J., and McGill, S. M., 2001, "Spinal shrinkage during repetitive controlled torsional, flexion and lateral bend motion exertions," *Ergonomics*, Vol. 44, No. 4, pp. 373-81.

Burr, D. B., Martin, R. B., Schaffler, M. B., and Radin, E. L., 1985, "Bone remodeling in response to in vivo fatigue microdamage," *Journal of Biomechanics*, Vol. 18, No. 3, pp. 189-200.

Burr, D. B., Schaffler, M. B., Yang, K. H., Lukoschek, M., Sivaneri, N., Blaha, J. D., and Radin, E. L., 1989a, "Skeletal change in response to altered strain environments: is woven bone a response to elevated strain?," *Bone*, Vol. 10, No. 3, pp. 223-33.

Burr, D. B., Schaffler, M. B., Yang, K. H., Wu, D. D., Lukoschek, M., Kandzari, D., Sivaneri, N., Blaha, J. D., and Radin, E. L., 1989b, "The effects of altered strain environments on bone tissue kinetics," *Bone*, Vol. 10, No. 3, pp. 215-21.

Buttermann, G. R., Kahmann, R. D., Lewis, J. L., and Bradford, D. S., 1991, "An experimental method for measuring force on the spinal facet joint: description and application of the method," *Journal of Biomechanical Engineering*, Vol. 113, No. 4, pp. 375-86.

Buttermann, G. R., Schendel, M. J., Kahmann, R. D., Lewis, J. L., and Bradford, D. S., 1992, "In vivo facet joint loading of the canine lumbar spine," *Spine*, Vol. 17, No. 1, pp. 81-92.

Cao, K. D., Grimm, M. J., and Yang, K. H., 2001, "Load sharing within a human lumbar vertebral body using the finite element method," *Spine*, Vol. 26, No. 12, pp. E253-60.

Cripton, P., Bruehlmann, S., Orr, T., Oxland, T., and Nolte, L., 2000, "In vitro axial preload application during spine flexibility testing: towards reduced apparatus- related artefacts.," *Journal of Biomechanics*, Vol. 33, No., pp. 1559-1568.

Davies, A. S., Tan, G. Y., and Broad, T. E., 1984, "Growth gradients in the skeleton of cattle, sheep and pigs," *Anatomia, Histologia, Embryologia: Veterinary Medicine Series C.*, Vol. 13, No. 3, pp. 222-30.

Frei, H., Oxland, T. R., and Nolte, L. P., 2002, "Thoracolumbar spine mechanics contrasted under compression and shear loading," *Journal of Orthopaedic Research*, Vol. 20, No. 6, pp. 1333-8.

Frei, H., Oxland, T. R., Rathonyi, G. C., and Nolte, L. P., 2001, "The effect of nucleotomy on lumbar spine mechanics in compression and shear loading," *Spine*, Vol. 26, No. 19, pp. 2080-9.

Graichen, F., Bergmann, G., and Rohlmann, A., 1996, "Patient monitoring system for load measurement with spinal fixation devices," *Medical Engineering and Physics*, Vol. 18, No. 2, pp. 167-74.

Gross, T. S., McLeod, K. J., and Rubin, C. T., 1992, "Characterizing bone strain distributions in vivo using three triple rosette strain gages," *Journal of Biomechanics*, Vol. 25, No. 9, pp. 1081-7.

Hongo, M., Abe, E., Shimada, Y., Murai, H., Ishikawa, N., and Sato, K., 1999, "Surface strain distribution on thoracic and lumbar vertebrae under axial compression. The role in burst fractures," *Spine*, Vol. 24, No. 12, pp. 1197-202.

Lanyon, L. E., and Rubin, C. T., 1984, "Static vs dynamic loads as an influence on bone remodelling," *Journal of Biomechanics*, Vol. 17, No. 12, pp. 897-905.

McLain, R. F., Yerby, S. A., and Moseley, T. A., 2002, "Comparative morphometry of L4 vertebrae: comparison of large animal models for the human lumbar spine," *Spine*, Vol. 27, No. 8, pp. E200-6.

Mikic, B., and Carter, D. R., 1995, "Bone strain gage data and theoretical models of functional adaptation," *Journal of Biomechanics*, Vol. 28, No. 4, pp. 465-9.

Mitchell, A. D., Scholz, A. M., and Pursel, V. G., 2001, "Total body and regional measurements of bone mineral content and bone mineral density in pigs by dual energy X-ray absorptiometry," *Journal of Animal Science*, Vol. 79, No. 10, pp. 2594-2604.

Miura, T., Panjabi, M., and Cripton, P., 2002, "A method to simulate in vivo cervical spine kinematics using in vitro compressive preload.," *Spine*, Vol. 27, No., pp. 43-48.

Nachemson, A., 1981, "Disc pressure measurements," *Spine*, Vol. 6, No., pp. 93-97.

Nasca, R. J., Lemons, J. E., Walker, J., and Batson, S., 1990, "Multiaxis cyclic biomechanical testing of Harrington, Luque, and Drummond implants," *Spine*, Vol. 15, No. 1, pp. 15-20.

Oda, T., and Panjabi, M. M., 2001, "Pedicle screw adjustments affect stability of thoracolumbar burst fracture," *Spine*, Vol. 26, No. 21, pp. 2328-33.

Oda, T., Panjabi, M. M., and Kato, Y., 2001, "The effects of pedicle screw adjustments on the anatomical reduction of thoracolumbar burst fractures," *European Spine Journal*, Vol. 10, No. 6, pp. 505-11.

Panjabi, M., 1988, "Biomechanical evaluation of spinal fixation devices. I. A conceptual framework," *Spine*, Vol. 13, No., pp. 1129-1134.

Panjabi, M., Abumi, K., Duranceau, J., and Crisco, J., 1988, "Biomechanical evaluation of spinal fixation devices. II. Stability provided by eight internal fixation devices," *Spine*, Vol. 13, No., pp. 1135-1140.

Panjabi, M., Miura, T., Cripton, P., Wang, J., Nain, A., and DuBois, C., 2001a, "Development of a system for in vitro neck muscle force replication in whole cervical spine experiments.," *Spine*, Vol. 26, No., pp. 2214-2219 S185.

Panjabi, M. M., 1998, "Cervical spine models for

biomechanical research," *Spine.*, Vol. 23, No. 24, pp. 2684-700.
Panjabi, M. M., Cholewicki, J., Nibu, K., Grauer, J. N., Babat, L. B., and Dvorak, J., 1998a, "Mechanism of whiplash injury," *Clinical Biomechanics*, Vol. 13, No. 4-5, pp. 239-249.
Panjabi, M. M., Kato, Y., Hoffman, H., and Cholewicki, J., 2001b, "Canal and intervertebral foramen encroachments of a burst fracture: effects from the center of rotation," *Spine*, Vol. 26, No. 11, pp. 1231-7.
Panjabi, M. M., Kato, Y., Hoffman, H., Cholewicki, J., and Krag, M., 2000, "A study of stiffness protocol as exemplified by testing of a burst fracture model in sagittal plane," *Spine*, Vol. 25, No. 21, pp. 2748-54.
Panjabi, M. M., Nibu, K., and Cholewicki, J., 1998b, "Whiplash injuries and the potential for mechanical instability," *European Spine Journal*, Vol. 7, No. 6, pp. 484-92.
Panjabi, M. M., Pearson, A. M., Ito, S., Ivancic, P. C., and Wang, J. L., 2004, "Cervical spine curvature during simulated whiplash," *Clin Biomech (Bristol, Avon)*, Vol. 19, No. 1, pp. 1-9.
Patwardhan, A., Havey, R., Ghanayem, A., Diener, H., Meade, K., Dunlap, B., and Hodges, S., 2000, "Load carrying capacity of the human cervical spine in compression is increased under a follower load," *Spine*, Vol. 25, No., pp. 1548-1554.
Patwardhan, A. G., Havey, R. M., Meade, K. P., Lee, B., and Dunlap, B., 1999, "A follower load increases the load-carrying capacity of the lumbar spine in compression," *Spine*, Vol. 24, No. 10, pp. 1003-9.
Patwardhan, A. G., Meade, K. P., and Lee, B., 2001, "A frontal plane model of the lumbar spine subjected to a follower load: implications for the role of muscles," *Journal of Biomechanical Engineering*, Vol. 123, No. 3, pp. 212-7.
Rikhraj, I. S., Tan, C. T., Tan, S. K., Teoh, S. H., and Hastings, G. W., 1999, "Use of titanium prosthesis to bridge a vertebral gap in the spine--a preliminary experimental study," *Annals of the Academy of Medicine, Singapore.*, Vol. 28, No. 1, pp. 20-4.
Rohlmann, A., Bergmann, G., and Graichen, F., 1994, "A spinal fixation device for in vivo load measurement," *Journal of Biomechanics*, Vol. 27, No. 7, pp. 961-7.
Rohlmann, A., Bergmann, G., Graichen, F., and Mayer, H. M., 1998, "Placing a bone graft more posteriorly may reduce the risk of pedicle screw breakage: analysis of an unexpected case of pedicle screw breakage," *Journal of Biomechanics*, Vol. 31, No. 8, pp. 763-7.
Rohlmann, A., Bergmann, G., Graichen, F., and Weber, U., 2000, "Changes in the loads on an internal spinal fixator after iliac-crest autograft," *Journal of Bone and Joint Surgery. British Volume*, Vol. 82, No. 3, pp. 445-9.
Rohlmann, A., Neller, S., Claes, L., Bergmann, G., and Wilke, H., 2001, "Influence of a follower load on intradiscal pressure and intersegmental rotation of the lumbar spine," *Spine*, Vol. 26, No., pp. E557-561.
Rubin, C. T., and Lanyon, L. E., 1984, "Regulation of bone formation by applied dynamic loads," *Journal of Bone and Joint Surgery*, Vol. 66, No. 3, pp. 397-402.
Shah, J. S., Hampson, W. G., and Jayson, M. I., 1978, "The distribution of surface strain in the cadaveric lumbar spine," *Journal of Bone and Joint Surgery. British Volume*, Vol. 60-B, No. 2, pp. 246-51.
Wilke, H., Wenger, K., and Claes, L., 1998, "Testing criteria for spinal implants: recommendations for the standardization of in vitro stability testing of spinal implants," *European Spine Journal*, Vol. 7, No., pp. 148-154.
Wilke, H. J., Kettler, A., and Claes, L. E., 1997, "Are sheep spines a valid biomechanical model for human spines?," *Spine*, Vol. 22, No. 20, pp. 2365-74.
Wilke, H. J., Krischak, S., and Claes, L., 1996, "Biomechanical comparison of calf and human spines," *Journal of Orthopaedic Research*, Vol. 14, No. 3, pp. 500-3.
Yoganandan, N., Cusick, J. F., Pintar, F. A., Droese, K., and Reinartz, J., 1994, "Cyclic compression-flexion loading of the human lumbar spine," *Spine*, Vol. 19, No. 7, pp. 784-90; discussion 791.